https://doi.org/10.1016/j.scitotenv.2019.133596

Deciphering source contributions of trace metal contamination in urban soil, road dust, and foliar dust of Guangzhou, southern China

Si-Yuan Liang[a], Jin-Li Cui[a, b], Xiang-Yang Bi[a, c], Xiao-San Luo[a, d], Xiang-Dong Li[a*]

[a]*Department of Civil and Environmental Engineering, The Hong Kong Polytechnic University, Hung Hom, Kowloon, Hong Kong*

[b]*Key Laboratory for Water Quality and Conservation of the Pearl River Delta, Ministry of Education; School of Environmental Science and Engineering, Guangzhou University, Guangzhou 510006, China*

[c]*State Key Laboratory of Biogeology and Environmental Geology, China University of Geosciences, Wuhan 430074, China*

[d]*International Center for Ecology, Meteorology, and Environment (IceMe), School of Applied Meteorology, Nanjing University of Information Science & Technology, Nanjing 210044, China*

Corresponding author (X.D. Li), E-mail address: cexdli@polyu.edu.hk (X.D. Li); Tel: (852) 2766 6041; Fax: (852) 2334 6389.

Abstract

Trace metal contamination prevails in various compartments of the urban environment. Understanding the roles of various anthropogenic sources in urban trace metal contamination is critical for pollution control and city development. In this study, the source contribution from various contamination sources to trace metal contamination (*e.g.*, Cu, Pb, Zn, Co, Cr and Ni) in different environmental compartments in a typical megacity, Guangzhou, southern China, was investigated using the receptor model (Absolute Principal Component Scores-Multiple Linear Regression, APCS-MLR) coupled with the Kriging technique. Lead isotopic data and APCS-MLR analysis identified industrial and traffic emissions as the major sources of trace metals in surface soil, road dust, and foliar dust in Guangzhou. Lead isotopic compositions of road dust and foliar dust exhibited similar ranges, implying their similar sources and potential metal exchange between them. Re-suspended soil contributed to 0–38% and 25-58% of the trace metals in the road dust and foliar dust, respectively, indicating the transport of the different terrestrial dust. Spatial distribution patterns implied that Cu in the road dust was a good indicator of traffic contamination, particularly with traffic volume and vehicle speed. Lead and Zn in foliar dust indicated mainly industrial contamination, which decreased from the emission source (*e.g.*, a power plant and steel factory) to the surrounding environment. The spatial influence of industry and traffic on the contamination status of road dust/foliar dust was successfully separated from that of other anthropogenic sources. This study demonstrated that anthropogenic inputs of trace metals in various environmental compartments (*e.g.*, urban soil, road dust, and foliar dust) can be evaluated using a combined APCS-MLR receptor model and geostatistical analysis at a megacity scale. The coupled use of APCS-MLR analysis, geostatistics, and Pb isotopes successfully deciphered the spatial influence of the contamination sources in the urban environment matrix, providing some important information for further land remediation and health risk assessment.

Keywords: Trace metals, Urban soil, Dust, Spatial distribution, Source appointment

1. Introduction

During recent decades, rapid urban development for modern human life requires various anthropogenic activities including industrial operations, municipal processes, construction activities, and traffic emissions [1, 2]. Subsequently, these anthropogenic activities have released considerable trace metals in various urban environmental compartments, including urban soil [3-5], road dust [6-8], and foliar dust [9, 10], which consequently have affected ecosystems and human health [11].

Trace metals in urban compartments are generally derived from multiple sources, such as the lithogenic matrix, atmospheric deposition, industrial activities, coal combustion, and traffic emissions [1, 4, 12, 13]. The various complex sources in urban areas contribute to the complexity of the contamination conditions. Urban soils are characterised by significant spatial heterogeneity from exogenous materials and geogenic matrix [3-5]. Road dust is primarily affected by road materials, traffic sources, and nearby industrial emissions [14]. As another environmental compartment, foliar dust includes falling particles from typical urban aerosols and other dust re-suspension [10, 15]. These urban compartments represent different sources for contaminants, and deciphering the quantitative contributions of contamination sources to the urban environment matrix is critical for their corresponding regulation and remediation.

To quantitatively identify metal input and separate the effect of a specific source, Pb isotopic signatures have been widely used to distinguish various Pb sources in urban environments [12, 16, 17] because of identical fingerprinting. Nevertheless, it is difficult to identify the exact contribution from complicated sources to other trace metals including Cu, Zn, etc. only using this method. The Absolute Principal Component Scores-Multiple Linear Regression (APCS-MLR) receptor model has been widely used to evaluate the source contribution of trace metals in fine particulate matter in air [18] and recently in urban soil [5, 19]. The APCS-MLR model enables source apportionment at each sampling location and the quantitative contributions of a

contaminant to each source group [20]. Elucidating the specific source for trace metal contamination at a city scale is critical for urban environmental management. However, elucidation of such a spatial pattern of anthropogenic contributions to trace metals in various environmental compartments, particularly in a megacity, remains unclear. Furthermore, whether there is any difference or acceptable suitability using different environmental compartments to explain trace metal contamination status in an urban area continues to need more evaluation. Therefore, based on previous studies [5, 18-20], we aimed to resolve the main contamination sources in an urban environment, and compare the suitability of soil, road dust, and foliar dust to describe urban contamination conditions in a typical megacity.

Guangzhou is a megacity in southern China, where industrial/traffic/agricultural activities have resulted in trace metal contamination in urban soil, road dust, plants, and aerosols to various extents [6, 21-25]. The objectives of the present study were to (1) investigate the trace metal concentration and distribution in the surface soil (0–3 cm), road dust, and foliar dust in Guangzhou and (2) spatially quantify the natural or anthropogenic contributions of trace metals using the APCS-MLR model, Kriging technique, and Pb isotopes. Clear spatial distribution of the prevailing contaminants (*e.g.*, traffic and industrial emissions) in urban environments can facilitate our understanding of the transport of metal pollutants among different environmental media.

2. Materials and methods

2.1. Study area and sample collection

Samples were collected in the city center of Guangzhou, China (22°26′–23°56′N, 112°57′–114°03′E) during November 2012. The sampling area covers approximately 200 km^2 and consists of typical industrial, commercial, and residential districts (Figure S1). The whole area was divided into 200 cells 1 km × 1 km in size, in which surface soil (0–3 cm, n=180), top soil (0–15 cm, n=180), road dust (n=178), and tree leaves (n=160) were collected. Generally, surface soil (*e.g.*, 0–3 cm) represents the soil

contamination status and affects oral ingestion and inhalation because it can be easily re-suspended [26]. Top soil at depths of 0–10 or 0–15 represents the mixed soil layers and is often used for assessing health risk [27]. In the present study, soil samples at each location were collected at 0–3 cm (surface soil) and at 0–15 cm (top soil) using a stainless-steel trowel. Each of the soil samples consisted of nine sub-samples obtained in a 2 m × 2 m grid. Road dust samples were obtained at a roadside near the soil sampling sites using a brush and dustpan. Tree leaves were collected from banyan trees (*Ficus microcarpa*), which can be found throughout Guangzhou. To maintain the consistency of the leaf samples, the heights of the sampled tree leaves ranged from 1.5 to 2 m. All of the samples were placed in polyethylene bags for transport and storage.

2.2. Sample preparation and analysis

Soil and road dust samples were dried in an oven at 60ºC for 3 days. Thereafter, they were crushed and sieved through a 2-mm polyethylene sieve to remove stones, coarse materials, and other debris. Leaf samples were divided into two batches: one washed by deionised water to eliminate foliar dust and one that was unwashed. Both the washed and unwashed leaf samples were dried in an oven at 60°C for 3 days. All the plant samples were ground into powder using a clean stainless-steel coffee grinder before analysis [22]. No contamination in the samples was observed from the grinder.

The prepared samples (0.20 g of soil, 0.10 g of road dust, and 1.00 g of tree leaves) were treated using a pseudo-total digestion method [3, 28]. Briefly, the samples were digested with concentrated HNO_3 and $HClO_4$ (4:1 (v/v) for soils and dust; 8:1 (v/v) for plants) in an aluminum heating block until dry, and then leached with 10 ml of 5% (v/v) HNO_3 at 70 ºC for 1 h. Finally, the total concentrations of metals were determined using inductively coupled plasma-atomic emission spectrometry (ICP-AES, Perkin Elmer Optima 3300DV). Quality assurance and quality control (QA/QC) were confirmed using standard reference materials including NIST SRM 2709a and ERM-CC141 (matrix for soil and road dust) and NIST SRM 1515 and 1573a (matrix for tree leaves), reagent blanks, and 10% replicates of the total samples. The recovery rates of the

majority elements for NIST SRM 2709a, ERM-CC141, NIST SRM 1515, and NIST SRM 1573a were approximately 80-118% except for some elements including Pb, Al, Cr, and Ni in some reference materials (Table S1), probably because of their low concentration and the absence of HF in the digestion process. The duplicate samples showed the bias was less than 5%.

2.3. Pb isotopic composition analysis

The Pb isotopic compositions of the selected soil, road dust, and tree leaves were measured using Inductively Coupled Plasma Mass Spectrometry (ICP-MS, Agilent Technologies 7700 series). An international standard reference material (NIST SRM 981, common lead) was used for sample calibration and QA/QC. The relative standard deviation (RSD) of the 100 replicates was generally less than 0.6%. The measured $^{204}Pb/^{207}Pb$, $^{206}Pb/^{207}Pb$, and $^{208}Pb/^{207}Pb$ ratios of NIST SRM 981 were 0.0646±0.0001, 1.0933±0.0017, and 2.3720±0.0018, respectively, which were in close agreement with the standard reference values of 0.0645, 1.0933, and 2.3704, respectively.

2.4. Calculation of trace metal concentrations in foliar dust

Trace metal concentrations in foliar dust can be estimated by the following equations:

$$C_{dust} \cdot (\rho_{dust} \cdot S_{leaf}) + C_{leaf} \cdot (\rho_{leaf} \cdot S_{leaf}) = C_{total} \cdot Mass_{total} \cdots\cdots(1)$$

$$Mass_{total} = \rho_{dust} \cdot S_{leaf} + \rho_{leaf} \cdot S_{leaf} \cdots\cdots(2)$$

Where C_{dust}, C_{total}, C_{leaf} are metal concentration in foliar dust, unwashed tree leaves, and washed tree leaves, respectively; $Mass_{total}$ is the mass of unwashed tree leaves; S_{leaf} is the area of leaf surface; ρ_{leaf} is leaf mass per unit area of leaf surface and was measured in the lab which approximated to 60.00 $g \cdot m^{-2}$; ρ_{dust} is foliar dust mass per unit area of leaf surface. ρ_{dust} is approximated to 1.16 $g \cdot m^{-2}$, the average maximum

dust-retention amount ($g \cdot m^{-2}$) on the same type of tree leaves (*Ficus microcarpa*) in commercial/traffic areas in Guangzhou [29]. Only one data was assigned to ρ_{dust} regardless the land use types, because almost all the samples were collected at roadsides, and variation from the land use types could be reduced during storage and transportation. It is important to note that the mass density of foliar dust under real-world conditions could be varied depending on the land use types. The calculated concentrations of Co, Cr, Cu, Ni, Pb, and Zn were 72%, 109%, 111%, 99%, 93%, and 73% of the corresponding metal concentrations of foliar dust measured by Zheng et al. [30] in Guangzhou.

2.5. Data analysis

An enrichment factor (EF), defined as the ratio of trace metal concentration in samples to the corresponding background concentration in Guangzhou [31], was used to estimate the anthropogenic influence on trace metal contamination in the soil and road dust [32]. An EF value less than 1 indicates that the source of trace metal is mainly of crustal origin or from natural weathering, while trace metals may originate from anthropogenic sources if the EF is greater than 1.

All the statistical analyses were conducted using PASW Statistic Version 18.0. Data were logarithm transformed to reduce the influence of high values prior to statistical analysis with details provided in the Supporting Information (SI). Principal component analysis (PCA) was conducted for source identification. The data set of surface soil, road dust, and foliar dust in the study was suitable for PCA with Bartlett test (p <0.01) and Kaiser-Meyer-Olkin (KMO) data ranging from 0.749 to 0.882, showing the data is suitable for Factor Analysis [33]. The receptor model APCS-MLR [19, 20] was used to estimate the contributions (%) of various anthropogenic sources to each metal in the urban soil, road dust, and foliar dust. The details of the receptor model (APCS-MLR) can be found in the SI.

2.6. Geostatistical analysis

The EFs of the trace metals in the surface soil and road dust, trace metals in foliar dust, factor scores from PCA, and source contributions (%) obtained from APCS-MLR were interpolated. The Kriging interpolation is the principal geostatistical technique to predict attribute values at un-sampled locations using information related to one or several attributes through capitalizing on the spatial correlation between the observations [34]. Semi-variogram (*e.g.*, spherical, Gaussian, and exponential model) was used in the interpolation to quantify the spatial variability between two points as a function of their distance. The selection of experimental variogram model and Kriging interpolation were conducted using ArcGIS 10.2 (ESRI Inc., USA).

3. Results and discussion

3.1. Trace metal concentrations in surface soil, road dust, and foliar dust

The concentrations of trace metals in the surface soil, road dust, and foliar dust are shown in Table 1. For the surface soil (0-3 cm), trace metals generally exhibited a significant correlation to that of the top soil (0–15 cm) (p <0.01, Table S2), showing their similar roles in identification of urban soil contamination. Because surface soil is more easily suspended into the air than topsoil for human inhalation and health risk [26, 35], only surface soil was discussed in the present study. Of the surface soils, a large number of samples exceeded the background values of the detected trace metals, including Co (76%), Cr (74%), Cu (97%), Ni (93%), Pb (69%), and Zn (93%), indicating a wide range of urban soil contamination in Guangzhou. Compared to other cities in China (Table S3), the metal concentrations in the urban soil in Guangzhou were generally lower than those in Shanghai [7] and Hong Kong [2], but higher than those in Beijing [36]. Compared to foreign countries, the concentration levels were lower than Athens (Greece) [37], but higher than Berlin (Germany) and Madrid (Spain) [38]. In comparison to metal concentrations in Denver (USA) [38] and Melbourne (Australia) [39], the concentrations of Pb and Zn were lower but the concentrations of Cr, Cu, and Ni were higher in Guangzhou.

The concentrations of Co, Cr, Cu, Ni, Pb, and Zn in different land use areas in Guangzhou are shown in Figure 1. Approximately 70–100% of the suburban samples, 73–97% of the institution/park samples, 67–96% of the residential samples, 54–96% of the commercial samples, 85–100% of the industrial samples, and 100% of the orchard samples exceeded the background value of Guangzhou. Specifically, trace metal concentrations from industrial and orchard areas were significantly (p <0.05) higher than those from other land use areas (Figure 1), showing severe trace metal contamination from anthropogenic activities in the urban environment, which need remediation before further land reuse. The results indicated that because of rapid urbanisation, the Guangzhou urban soil has been contaminated to a different extent depending on the land use, as is often the case for industrial and urban development in many regions such as Hong Kong [2], Shanghai [7], Beijing [36], Melbourne [39], Athens [40], and New York [41].

Trace metal concentrations in road dust are shown in Table 1. Comparing to the nearby corresponding soil samples, most of the road dust showed higher trace metal concentrations, particularly for Cu, Zn, and Pb (Table 1), consistent with a previous publication [7]. After transforming metal concentrations to EF values compared to the background value (Table S4), we observed much higher EF values of Cu (median value at 7.7) and Zn (median value at 6.3) in road dust, suggesting their specific traffic origin, probably from brake abrasion and tire wear [2, 11, 42]. The road dust samples generally showed a black colour, suggesting brake abrasion and tire debris products. Various traffic conditions including traffic volume and speed considerably affect trace metal concentration levels if considering the traffic source as the primary contribution source [14]. By grouping the samples based on traffic volume and speed [43], it was found that the concentrations of Cu and Zn in road dust slightly increased with the increasing traffic volume (Figure S2). Some studies have reported that a high occurrence of braking on a road, particularly during heavily congested traffic periods, produces more Cu/Zn/Pb contamination in road dust [44, 45]. The effect of traffic speed on trace metal variation was not obvious (Figure S3). Interestingly for the Pb concentration in road

dust, no significant effect was observed by traffic volume and speed possibly because of the use of lead-free petrol in Guangzhou since 1997. Therefore, considering the relation of Cu/Zn to traffic conditions, Cu/Zn levels may be considered as an environmental marker for traffic sources during recent years rather than Pb.

In addition to traffic factors, we observed increasing concentrations of trace metals including Cr, Cu, Pb, and Zn in road dust in the industrial area, suggesting considerable influence of industrial sources on road dust (Figure 1). Other factors such as urban waste during transportation; city construction and building restoration; the use of pesticides, fertilisers, and medical devices; plant fragments from nearby vegetation; and soil-originated deposits may also result in contamination to road dust, making the contamination sources more complex [8, 42, 46].

Trace metal concentrations in tree leaves and foliar dust are shown in Table 1. For tree leaves, trace metal concentrations in the washed samples showed significant differences (p <0.05) in comparison to those of the unwashed samples, suggesting deposited trace metals on the leaf surface from suspended soil particles and atmospheric particular matter [9]. Foliar dust in the industrial region showed relatively higher concentrations of trace metals than those from the other land use areas (Figure 1) with significance for Pb (p <0.05), showing deposition of atmospheric particles from industrial sources. Correspondingly, trace metals in the foliar dust decreased with increasing distance from the emission source (*e.g.*, a power plant and steel factory), as identified by Pb and Zn with significant difference (p <0.05, Figure 2).

3.2. Spatial distribution of trace metals in surface soil, road dust, and foliar dust

A distribution map was developed for each trace metal in each environmental compartment (Figure 3 for Cu, Pb, Zn; and Figure S4 for Co, Cr, Ni). In the surface soils, high concentrations of trace metals were observed near a steel factory (southwest Guangzhou, Figure 3 a-c) and around the orchards (south Guangzhou, Figure 3 a-c). Trace metal contamination at similar sites has been reported in previous studies [22,

47]. The high concentrations around the power plant were possibly caused by coal combustion, and other typical urban emissions, such as traffic sources [11, 48].

In the road dust, the trace metal distribution patterns are shown in Figure 3 d-f (Cu, Pb, and Zn) and Figure S4 d-f (Co, Cr, and Ni) with clear spatial heterogeneity. High concentrations of Cu, Zn, Ni, and Pb were found in the area with high density of major roads and heavily congested traffic (shown with high traffic volumes (Figure S5) and low vehicular speed (Figure S6)). Hot spots of Pb, Zn, Cr, and Co were also found in areas near the industrial sites, such as the steel factory to the southwest, brickyard, and some chemical industrial sites to the northeast, suggesting industrial influence on the road dust. In addition, the intensive traffic volume for industrial transport and the frequent brake abrasion and stop-start maneuvers during loading/unloading often produce a high amount of trace metals in industrial regions [6, 14]. It was demonstrated that driving conditions, such as heavy load applied on the tire surface and harsh braking, could increase the emission of tire wear particles which contained a large amount of trace metals, particularly Zn [49].

Foliar dust generally showed similar distribution patterns of trace metals to those of surface soil (Figure 3 g-i for Cu, Pb, Zn; and Figure S4 g-i for Co, Cr, Ni), with hot spots around the power plant and the southwest and northeast areas where industrial activities prevail. Consistently, Liu et al. [29] found the highest dust accumulation on leaves collected in the industrial areas of Guangzhou and a significant accumulation of dust deposits on leaves was also found in industrial regions of a city in Italy [10]. It has been reported that gravity or wind impacts contribute to atmospheric dust deposits on leaves [10, 15]; therefore, foliar dust can reflect nearby contamination sources. Trace metal concentrations (mg kg^{-1}) in foliar dust varied with a decreasing order of Zn (744) > Cu (223) > Pb (216) > Cr (129) > Ni (40.8) > Co (8.09). This decreasing trend among metals of foliar dust was similar to that of the Guangzhou atmospheric dry depositional fluxes (mg/m^2/yr, Zn (54.1) > Cu (9.77) > Cr (6.53) > Ni (3.01) > Co (0.48)) [50], indicating that trace metal concentrations in foliar dust were close associated with

atmospheric dry deposition.

3.3. Source identification using Pb isotopic compositions

Lead isotopes were analyzed to identify the potential sources of trace metals, particularly Pb, in surface soil, road dust, and foliar dust (Figure 4). Generally, surface soil showed much higher $^{206}Pb/^{207}Pb$ and $^{208}Pb/^{207}Pb$ ratios compared to those in road dust, foliar dust, and $PM_{2.5}$ [51]. Similar scopes of Pb isotopic compositions were found in road dust, foliar dust, and $PM_{2.5}$, showing similar Pb sources and possible transport between each other.

Lead isotopic compositions in surface soils were 1.1699–1.2039 for the $^{206}Pb/^{207}Pb$ ratio and 2.4506–2.4934 for the $^{208}Pb/^{207}Pb$ ratio (Table 2 and Figure 4). The Pb isotopic compositions fell within a range of local traffic/industrial/coal sources and background values in Guangzhou (Table S5-S6) [16, 24, 52-56], showing mixing sources contributed to Pb contamination in urban soils. The higher Pb concentrations in soil were linked to the lower $^{206}Pb/^{207}Pb$ and $^{208}Pb/^{207}Pb$ ratios (Figure S7), and thus the heavier contaminated soils had Pb isotopic compositions ($^{206}Pb/^{207}Pb$ and $^{208}Pb/^{207}Pb$) closer to the vehicular and industrial emission sources. Specifically, the industrial sites contributed to the nearby surface soil, with a decreasing pattern of Pb isotopic ratios ($^{206}Pb/^{207}Pb$ and $^{208}Pb/^{207}Pb$) in some samples from industrial sites.

For road dust, the Pb isotopic compositions ($^{206}Pb/^{207}Pb$ and $^{208}Pb/^{207}Pb$) were in the region between the unleaded gasoline, leaded gasoline, industrial sources, and urban soils (Figure 4, Table S5-S6). Historically used gasoline with Pb additives significantly contributed to Pb in the Guangzhou road dust before the phase-out of leaded gasoline and even several years thereafter [57]. Nevertheless, in the present study, a significant linear correlation between $^{206}Pb/^{207}Pb$ and $^{208}Pb/^{207}Pb$ (R^2=0.96) was found in road dust samples and unleaded gasoline used in Chinese cities (Figure 4). Additionally, an overlap of Pb isotopic compositions ($^{206}Pb/^{207}Pb$ and $^{208}Pb/^{207}Pb$) was observed between road dust samples and unleaded gasoline samples (Figure 4). As shown in Figure S7, the Pb isotopic ratios ($^{206}Pb/^{207}Pb$ and $^{208}Pb/^{207}Pb$) of road dust were higher

than those of soils with significant difference (p <0.05 for $^{206}Pb/^{207}Pb$; p <0.01 for $^{208}Pb/^{207}Pb$), demonstrating the different sources of Pb between road dust and urban soils. Furthermore, the level of Pb contamination of road dust was negatively linked to the Pb isotopic ratios ($^{206}Pb/^{207}Pb$ and $^{208}Pb/^{207}Pb$) (Figure S7). Because a small amount of Pb (60–280 μg/L) remains in unleaded gasoline in China [17], this negative correlation highlighted the significance of unleaded gasoline (with lower Pb isotopic ratios) on Pb contamination in the road dust. Similarly, vehicle exhaust from unleaded gasoline and diesel fuels has been reported as a major source of Chinese road dust after the prohibition of leaded gasoline in Beijing [4] and Nanjing [12]. The combined results indicated that the major Pb sources of road dust were from unleaded gasoline. In the industrial regions with heavier Pb contamination of road dust, the Pb isotopic compositions of the road dust differed from those of the industrial sources but were near those of unleaded gasoline. Intensive vehicular traffic for industrial transport could cause an increase in the Pb concentration in industrial road dust [6, 14]. Our results indicated that heavy-duty vehicles for industrial transport instead of direct industrial emissions could largely contribute to the Pb contamination of road dust in industrial regions.

For tree leaves (Figure 4 and Table 2), the unwashed leaves showed values of 1.1677–1.1738 for the $^{206}Pb/^{207}Pb$ ratio and 2.4416–2.4633 for the $^{208}Pb/^{207}Pb$ ratio; the corresponding washed leaves showed values of 1.1670–1.1762 for the $^{206}Pb/^{207}Pb$ ratio and 2.4357-2.4645 for the $^{208}Pb/^{207}Pb$ ratio. The Pb isotopic compositions of the washed leaves generally fell within the range between unwashed leaves/$PM_{2.5}$ and soils, but were much nearer unwashed leaves/$PM_{2.5}$, in line with studies conducted in Shanghai [58], Nanjing [59], the North Pennines of the United Kingdom [60], and Biesbosch National Park in the Netherlands [61]. The Pb isotopic ratios ($^{206}Pb/^{207}Pb$ and $^{208}Pb/^{207}Pb$) of the leaves were obviously less than those of the soils, probably because 1) the mobile/bioavailable/bioaccessible fractions of the soil had Pb isotopic ratios ($^{206}Pb/^{207}Pb$ and $^{208}Pb/^{207}Pb$) nearer those of anthropogenic sources [27, 62, 63] and thus the plants preferentially took up more labile anthropogenic Pb forms [64], and 2)

Pb in the plant leaves was primarily a function of foliar uptake from atmospheric deposition [58, 60] as supported by the similarity of the Pb isotopic compositions in the unwashed leaves/$PM_{2.5}$ and leaves. Based on the calculation process of trace metal concentrations (section 2.4), it was estimated that the Pb isotopic compositions ($^{206}Pb/^{207}Pb$ and $^{208}Pb/^{207}Pb$) in the unwashed leaves were the mixed results from those in the corresponding foliar dust and washed leaves. By comparing the Pb isotopic compositions ($^{206}Pb/^{207}Pb$ and $^{208}Pb/^{207}Pb$) between the washed and the corresponding unwashed leaf samples in Table S6, the possible Pb isotopic compositions ($^{206}Pb/^{207}Pb$ and $^{208}Pb/^{207}Pb$) of foliar dust were estimated and circled in red in Figure 4, which were similar to those of the Guangzhou $PM_{2.5}$ particles, and within the range of the industrial sources and traffic exhaust. The comparison results indicated air particle deposition on tree leaves from nearby contamination sources. Furthermore, the unwashed leaf samples from the industrial contaminated regions showed a Pb isotopic composition encircling the industrial sources, showing the industrial influence on nearby foliar dust. It should be noted that the Pb isotopic compositions of an unwashed leaf sample from a construction site showed different Pb isotopic compositions. Thus, construction activities may also alter the Pb isotopic signatures of the foliar dust.

3.4. Source apportionment using APCS-MLR and its spatial variation

The aforementioned analysis indicated that there were primarily two sources contributing to the urban soil contamination: industry and traffic. Nevertheless, the exact contribution extent of various contamination sources to these trace metals in each urban compartment is not clear, which is critical for further environmental assessment and remediation. Therefore, statistical PCA (Table S7) and APCS-MLR (Table S8) were employed to identify the composite contribution to the urban environmental matrix. Compared to geogenic influences, the anthropogenic contributions accounted for a much higher percentage of trace metals, particularly for Cu, Pb, and Zn in all the compartments (Table S8).

PCA analysis indicated three components, accounting for 69–89% of the total

variance of the data (Table S7). The factor scores of each component were interpolated for source identification according to previous studies [65, 66] as shown in Figure S8. In the surface soil, the first component (PC1) was composed of Cr, Mn, and Ni and the second component (PC2) Cu, Pb, and Zn. Approximately 65–97% of these elements in these PCs (PC1 and PC2) showed EF values higher than 1. PC1 exhibited two hot spots around a steel factory and orchards, and high loadings of PC2 were mainly located in the industrial areas, around the power plant, and at roadsides with high traffic volumes (Figure S8 a-b), indicating their anthropogenic industrial, traffic, and agricultural sources. Quantitative analysis using APCS-MLR indicated that anthropogenic sources (PC1 and PC2) accounted for 80% of the Cu, 58% of the Pb, and 78% of the Zn contamination in surface soils. The average anthropogenic contribution (PC1 and PC2) of Cu, Pb, and Zn in the urban soils decreased in the order of industrial sites (70–85%) >high traffic sites (61–81%) >low traffic sites (57–79%) (Table S9). In particular, the anthropogenic contribution to Cu, Pb and Zn in urban soils of industrial sites showed significant difference (p <0.05) with those of other sites. The results were generally in line with the Pb isotopic analysis, indicating that the Cu, Pb, and Zn contamination in the Guangzhou urban environment is mainly caused by anthropogenic influence and urban soil was a good indicator of the development a city. The third component (PC3) was associated with Co, Al, and Fe with low EFs (0.2–1.4) and should be classified as background lithogenic sources [65].

In the road dust, PC1 was composed of Co, Cr, Fe, Mn, Pb, and Zn with EF values of 1.1–6.9, showing hot spots in industrial areas and some major roads with high traffic volumes (Figure S8 d), which contributed as the major sources in road dust. The APCS-MLR model indicated that 71±12% of the Pb and 48±14% of the Zn was derived from industrial activities and heavy traffic (PC1) all over the urban area (Table S8). PC2 included Cu and Ni, with extremely high Cu (10.3) and Ni (2.0) EF values. The major hot spot (Figure S8 e) was coincided with high traffic volumes (Figure S5), major road systems, and heavily congested traffic as indicated by the low vehicular speed (Figure S6). Other high factor loadings of PC2 were also overlapped with high traffic volumes

shown in Figure S5. These results indicated the major contribution of traffic emissions to PC2, which is consistent given that Cu and Ni mainly originate from exhaust emissions and brake abrasion [3, 14, 67]. The direct traffic sources (PC2) (Figure 5) contributed to 100% of the Cu, 40–50% of the Pb, and 50–60% of the Zn in road dust in the area with highest population density [43] and dense traffic network (Figure S6). This was in line with the concentration levels that trace metals, particularly Cu, increased because of heavily congested traffic. Thus, the spatial distribution of the traffic impacts was clearly represented by PC2 in the road dust and Cu may be a possible indicator of road dust contamination. PC3 in the road dust included only Al with a low EF value (0.1–0.7), suggesting a source of soil matrix to road dust.

In foliar dust, Al, Fe, and Pb together constituted PC1 and were attributed to local coal combustion and other industrial emissions [68], as supported by the overlap between the hot spots and known industrial activities (Figure S8 g). The contribution of industrial sources (PC1) to trace metals in foliar dust increased in the hot spots around the power plant and industrial districts (Figure 5). As shown by the Pb and Zn concentrations in Figure 2, significant influence from such emissions was highest near the emission sources and gradually decreased as the plume dispersed [69] (p <0.05). Thus, the spatial industrial influence was clearly exhibited by the distribution of PC1 in the foliar dust. PC2 was composed of Cu, Zn and Cr, with hot spots located at roadside sites under overpasses (Figure S8 h), indicating the traffic contribution of PC2. The gravity and wind impacts could contribute to traffic dust from overpasses deposited on plant leaves. Traffic contributions (PC2) contributed to more than 40% of the Cu and Zn, and 16-56% of the Pb in foliar dust next to overpasses (Figure S11 d-f). Cobalt and Ni comprised PC3, and were attributed mainly to soil re-suspension, according to the similar concentrations of Co between surface soils and foliar dust (Table 1). Chromium and Ni revealed similar moderate loadings on different PCs (Table S7), indicating the multiple source influence on their distribution.

3.5 Implications on trace metal cycling, contamination indicators, and health risk

assessment in urban environment

Trace metals in a megacity spread from various anthropogenic sources to environmental compartments, and there is exchange between them (Figure 6). Pairwise correlations among surface soil, road dust, and foliar dust were found for Pb and Zn (Table S2), reflecting the similar responses among these environmental compartments to Pb and Zn sources. Industrial emissions were identified as a major source for trace metal contamination in the Guangzhou urban environment. At a citywide scale (Figure 5) and zooming in on industrial regions (Figure 2), our study showed the spatial industrial influence on foliar dust with an affecting distance of approximately 3 to 4 km, similar to studies conducted of soils [70-72]. However, soil metals were not negatively correlated with the distance from the sources in our study probably because of more varied sources in the urban soils [71]. As another important source of trace metals, the traffic influence on road dust decreased along with the distance from the city center at a city scale (Figure 5). Studies [73-75] reported that the traffic influence on soil metals was generally limited from 3 to 250 m, although it was not clearly shown in our study using a 1 km × 1 km sampling density. The compartmental comparisons demonstrated the different suitability of soil, road dust, and foliar dust in describing different types of urban contamination sources. This may facilitate the selection of a contamination indicator for environmental assessment before performing a specific land remediation and creating informed guidelines for pollution control.

In urban environments, trace metals are transported from these sources to terrestrial compartments via dry and wet deposition, while the resuspension of terrestrial dust also contributes considerable trace metals to nearby compartments [46]. For example, re-suspended soil contributed 0–38% and 25-58% of the trace metals in the Guangzhou road dust and foliar dust, respectively (Table S8). Our previous work [24] also demonstrated that finer-grained particles of soil dust were more sensitive to anthropogenic Pb sources and had a higher resuspension ability as compared to bulk soil. Therefore, the health risk from terrestrial dust, such as soil dust and road dust,

should be considered around industrial areas and some sensitive regions such as orchards, where children playing should be avoided and workers should be protected from inhalation by a mask while working.

Conclusion

Our systematic geochemical survey of soil, road dust, and foliar dust in the megacity Guangzhou showed that trace metal contamination was mainly affected by local industrial and traffic activities. An industrial influence was clearly exhibited by the Pb and Zn in foliar dust, and the Cu content in road dust was a good indicator of traffic contamination. Re-suspended soil contributed 0–38% and 25-58% of the trace metals in the Guangzhou road dust and foliar dust, respectively, indicating the transport of the different terrestrial dust. The plots of the $^{206}Pb/^{207}Pb$ vs. $^{208}Pb/^{207}Pb$ ratios implied similar Pb sources for road dust and foliar dust, and potential transport of Pb between these environmental compartments in the urban environment. Using combined APCS-MLR analysis, geostatistics, and Pb isotopes, we successfully deciphered the spatial influence of contamination sources in the urban environment matrix, providing important information for further land remediation and health risk assessment.

Acknowledgements

Funding for this research was provided by the Hong Kong Polytechnic University and Natural Science Foundation of China (NFSC 41603093 and 41273003). We thank the students of the China University of Geoscience and The Hong Kong Polytechnic University for their assistance on field sampling and sample preparation.

Appendix A. Supplementary data

Supplementary data related to this article can be found at http://

Reference

(1) Alloway, B. J. *Heavy metals in soils*. Springer Netherlands: 2013; p 1.

(2) Li, X. D.; Poon, C. S.; Liu, P. S. Heavy metal contamination of urban soils and street dusts in Hong Kong. *Appl. Geochem.* **2001,** *16*, 1361-1368.

(3) Li, X. D.; Lee, S. L.; Wong, S. C.; Shi, W. Z.; Thornton, I. The study of metal contamination in urban soils of Hong Kong using a GIS-based approach. *Environ. Pollut.* **2004,** *129*, 113-124.

(4) Yu, Y.; Li, Y. X.; Li, B.; Shen, Z. Y.; Stenstrom, M. K. Metal enrichment and lead isotope analysis for source apportionment in the urban dust and rural surface soil. *Environ. Pollut.* **2016,** *216*, 764-772.

(5) Yang, Y.; Christakos, G.; Guo, M.; Xiao, L.; Huang, W. Space-time quantitative source apportionment of soil heavy metal concentration increments. *Environ. Pollut.* **2017,** *223*, 560-566.

(6) Duzgoren-Aydin, N. S.; Wong, C. S. C.; Aydin, A.; Song, Z.; You, M.; Li, X. D. Heavy metal contamination and distribution in the urban environment of Guangzhou, SE China. *Environ. Geochem. Health* **2006,** *28*, 375-391.

(7) Shi, G. T.; Chen, Z. L.; Xu, S. Y.; Zhang, J.; Wang, L.; Bi, C. J.; Teng, J. Y. Potentially toxic metal contamination of urban soils and roadside dust in Shanghai, China. *Environ. Pollut.* **2008,** *156*, 251-260.

(8) Men, C.; Liu, R.; Xu, F.; Wang, Q.; Guo, L.; Shen, Z. Pollution characteristics, risk assessment, and source apportionment of heavy metals in road dust in Beijing, China. *Sci. Total Environ.* **2018,** *612*, 138-147.

(9) Deljanin, I.; Antanasijević, D.; Bjelajac, A.; Urošević, M. A.; Nikolić, M.; Perić-Grujić, A.; Ristić, M. Chemometrics in biomonitoring: Distribution and correlation of trace elements in tree leaves. *Sci. Total Environ.* **2016,** *545–546*, 361-371.

(10) Sgrigna, G.; Sæbø, A.; Gawronski, S.; Popek, R.; Calfapietra, C. Particulate matter deposition on Quercus ilex leaves in an industrial city of central Italy. *Environ. Pollut.* **2015,** *197*, 187-194.

(11) Li, G.; Sun, G. X.; Ren, Y.; Luo, X. S.; Zhu, Y. G. Urban soil and human health: a review. *Eur. J. Soil Sci.* **2018,** *69*, 196-215.

(12) Hu, X.; Sun, Y. Y.; Ding, Z. H.; Zhang, Y.; Wu, J. C.; Lian, H. Z.; Wang, T. J. Lead contamination and transfer in urban environmental compartments analyzed by lead levels and isotopic compositions. *Environ. Pollut.* **2014,** *187*, 42-48.

(13) Cui, J. L.; Zhao, Y. P.; Li, J. S.; Beiyuan, J. Z.; Tsang, D. C. W.; Poon, C. S.; Chan, T. S.; Wang, W. X.; Li, X. D. Speciation, mobilization, and bioaccessibility of arsenic in geogenic soil profile from Hong Kong. *Environ. Pollut.* **2018,** *232*, 375-384.

(14) Duong, T. T. T.; Lee, B. K. Determining contamination level of heavy metals in road dust from busy traffic areas with different characteristics. *J. Environ. Manage.* **2011,** *92*, 554-562.

(15) Song, Y. S.; Maher, B. A.; Li, F.; Wang, X. K.; Sun, X.; Zhang, H. X. Particulate matter deposited on leaf of five evergreen species in Beijing, China: Source identification and size distribution. *Atmos. Environ.* **2015,** *105*, 53-60.

(16) Zhao, Z. Q.; Zhang, W.; Li, X. D.; Yang, Z.; Zheng, H. Y.; Ding, H.; Wang, Q. L.; Xiao, J.; Fu, P. Q. Atmospheric lead in urban Guiyang, Southwest China: Isotopic source signatures. *Atmos. Environ.* **2015,** *115*, 163-169.

(17) Bi, X. Y.; Li, Z. G.; Wang, S. X.; Zhang, L.; Xu, R.; Liu, J. L.; Yang, H. M.; Guo, M. Z. Lead isotopic compositions of selected coals, Pb/Zn ores and fuels in China and the application for source tracing. *Environ. Sci. Technol.* **2017,** *51*, 13502-13508.

(18) Thurston, G. D.; Ito, K.; Lall, R. A source apportionment of U.S. fine particulate matter air

pollution. *Atmos. Environ.* **2011,** *45*, 3924-3936.

(19) Luo, X. S.; Xue, Y.; Wang, Y. L.; Cang, L.; Xu, B.; Ding, J. Source identification and apportionment of heavy metals in urban soil profiles. *Chemosphere* **2015,** *127*, 152-157.

(20) Thurston, G. D.; Spengler, J. D. A quantitative assessment of source contributions to inhalable particulate matter pollution in metropolitan Boston. *Atmos. Environ.* **1985,** *19*, 9-25.

(21) Lee, C. S. L.; Li, X. D.; Zhang, G.; Li, J.; Ding, A. J.; Wang, T. Heavy metals and Pb isotopic composition of aerosols in urban and suburban areas of Hong Kong and Guangzhou, South China-Evidence of the long-range transport of air contaminants. *Atmos. Environ.* **2007,** *41*, 432-447.

(22) Bi, X. Y.; Liang, S. Y.; Li, X. D. Trace metals in soil, dust, and tree leaves of the urban environment, Guangzhou, China. *Chin. Sci. Bull.* **2013,** *58*, 222-230.

(23) Lu, Y.; Yin, W.; Zhu, F.; Zhang, G. L. The spatial distribution and sources of metals in urban soils of Guangzhou, China. *19th world congress of soil science, soil solutions for a changing world Brisbane, Australia* **2010**.

(24) Bi, X. Y.; Liang, S. Y.; Li, X. D. A novel *in situ* method for sampling urban soil dust: Particle size distribution, trace metal concentrations, and stable lead isotopes. *Environ. Pollut.* **2013,** *177*, 48-57.

(25) Gu, Y. G.; Gao, Y. P.; Lin, Q. Contamination, bioaccessibility and human health risk of heavy metals in exposed-lawn soils from 28 urban parks in southern China's largest city, Guangzhou. *Appl. Geochem.* **2016,** *67*, 52-58.

(26) Acosta, J. A.; Cano, A. F.; Arocena, J. M.; Debela, F.; Martínez-Martínez, S. Distribution of metals in soil particle size fractions and its implication to risk assessment of playgrounds in Murcia City (Spain). *Geoderma* **2009,** *149*, 101-109.

(27) Luo, X. S.; Yu, S.; Li, X. D. The mobility, bioavailability, and human bioaccessibility of trace metals in urban soils of Hong Kong. *Appl. Geochem.* **2012,** *27*, 995-1004.

(28) Cui, J. L.; Luo, C. L.; Tang, C. W. Y.; Chan, T. S.; Li, X. D. Speciation and leaching of trace metal contaminants from e-waste contaminated soils. *J. Hazard. Mater.* **2017,** *329*, 150-158.

(29) Liu, L.; Guan, D. S.; Peart, M. R.; Wang, G.; Zhang, H.; Li, Z. W. The dust retention capacities of urban vegetation—a case study of Guangzhou, South China. *Environ. Sci. Pollut. R.* **2013,** *20*, 6601-6610.

(30) Zheng, Y. M.; Gao, Q. Z.; Wen, X. H.; Yang, M.; Chen, H. D.; Wu, Z. Q.; Lin, X. H. Multivariate statistical analysis of heavy metals in foliage dust near pedestrian bridges in Guangzhou, South China in 2009. *Environ. Earth Sci.* **2013,** *70*, 107-113.

(31) Guangdong Geological Survey *Multi-purposes geochemical survey: Pear River Delta, Guangdong province*; 2010.

(32) Manta, D. S.; Angelone, M.; Bellanca, A.; Neri, R.; Sprovieri, M. Heavy metals in urban soils: a case study from the city of Palermo (Sicily), Italy. *Sci. Total Environ.* **2002,** *300*, 229-243.

(33) Zhang, W. SPSS11 statistical analysis (Advanced). In Beijing: Hope Electronic Press: 2002.

(34) Wackernagel, H. *Multivariate geostatistics*. Springer Science & Business Media: 2003.

(35) Miguel, E. D.; Jiménez, d. G., M; Llamas, J. F.; Martíndorado, A.; Mazadiego, L. F. The overlooked contribution of compost application to the trace element load in the urban soil of Madrid (Spain). *Sci. Total Environ.* **1998,** *215*, 113-122.

(36) Liu, R.; Wang, M. E.; Chen, W. P.; Peng, C. Spatial pattern of heavy metals accumulation risk in urban soils of Beijing and its influencing factors. *Environ. Pollut.* **2016,** *210*, 174-181.

(37) Kelepertzis, E.; Argyraki, A. Geochemical associations for evaluating the availability of potentially harmful elements in urban soils: Lessons learnt from Athens, Greece. *Appl. Geochem.* **2015,**

574 *59*, 63-73.
575 (38) Johnson, C. C.; Demetriades, A.; Locutura, J.; Ottesen, R. T. *Mapping the chemical environment*
576 *of urban areas*. Wiley Online Library: 2011.
577 (39) Laidlaw, M. A. S.; Alankarage, D. H.; Reichman, S. M.; Taylor, M. P.; Ball, A. S. Assessment of
578 soil metal concentrations in residential and community vegetable gardens in Melbourne, Australia.
579 *Chemosphere* **2018,** *199*, 303-311.
580 (40) Argyraki, A.; Kelepertzis, E. Urban soil geochemistry in Athens, Greece: The importance of local
581 geology in controlling the distribution of potentially harmful trace elements. *Sci. Total Environ.* **2014,**
582 *482-483*, 366-377.
583 (41) Burt, R.; Hernandez, L.; Shaw, R.; Tunstead, R.; Ferguson, R.; Peaslee, S. Trace element
584 concentration and speciation in selected urban soils in New York City. *Environ. Monit. Assess.* **2014,** *186*,
585 195-215.
586 (42) Rogge, W. F.; Hildemann, L. M.; Mazurek, M. A.; Cass, G. R.; Simoneit, B. R. Sources of fine
587 organic aerosol. 3. Road dust, tire debris, and organometallic brake lining dust: roads as sources and
588 sinks. *Environ. Sci. Technol.* **1993,** *27*, 1892-1904.
589 (43) Guangzhou Transport Planning Research Institute Guangzhou transport development annual
590 report. **2012**.
591 (44) Sahu, R.; Elumalai, S. P. Identifying speed hump, a traffic calming device, as a hotspot for
592 environmental contamination in traffic-affected urban roads. *ACS Omega* **2017,** *2*, 5434-5444.
593 (45) Harrison, R. M.; Jones, A. M.; Gietl, J.; Yin, J.; Green, D. C. Estimation of the contributions of
594 brake dust, tire wear, and resuspension to nonexhaust traffic particles derived from atmospheric
595 measurements. *Environ. Sci. Technol.* **2012,** *46*, 6523-6529.
596 (46) Charlesworth, S.; De Miguel, E.; Ordóñez, A. A review of the distribution of particulate trace
597 elements in urban terrestrial environments and its application to considerations of risk. *Environ. Geochem.*
598 *Health* **2011,** *33*, 103-123.
599 (47) Li, J. T.; Qiu, J. W.; Wang, X. W.; Zhong, Y.; Lan, C. Y.; Shu, W. S. Cadmium contamination in
600 orchard soils and fruit trees and its potential health risk in Guangzhou, China. *Environ. Pollut.* **2006,** *143*,
601 159-165.
602 (48) Luo, X. S.; Yu, S.; Zhu, Y. G.; Li, X. D. Trace metal contamination in urban soils of China. *Sci.*
603 *Total Environ.* **2012,** *421-422*, 17-30.
604 (49) Kim, G.; Lee, S. Characteristics of tire wear particles generated by a tire simulator under various
605 driving conditions. *Environ. Sci. Technol.* **2018**.
606 (50) Huang, W.; Duan, D. D.; Zhang, Y. L.; Cheng, H. F.; Ran, Y. Heavy metals in particulate and
607 colloidal matter from atmospheric deposition of urban Guangzhou, South China. *Mar. Pollut. Bull.* **2014,**
608 *85*, 720-726.
609 (51) Ming, L. L. Fine atmospheric particles ($PM_{2.5}$) in large city clusters, China: Chemical
610 compositions, temporal-spatial variations and regional transport. The Hong Kong Polytechnic University,
611 2016.
612 (52) Li, Y. G.; Lu, Y. F. Lead isotopes as a tracer of tea Pb contamination in the west lake tea plantation.
613 *Geophysical and Geochemical Exploration* **2008,** *32*, 180-185. in Chinese.
614 (53) Gao, Z. Y.; Yin, G.; Ni, S. J.; Zhang, C. J. Geochemical feature of the urban environmental lead
615 isotope in Chengdu city. *Carsologica. Sinica.* **2004,** *23*, 267-272. in Chinese.
616 (54) Zheng, J.; Tan, M.; Shibata, Y.; Tanaka, A.; Li, Y.; Zhang, G.; Zhang, Y.; Shan, Z. Characteristics
617 of lead isotope ratios and elemental concentrations in PM_{10} fraction of airborne particulate matter in

618 Shanghai after the phase-out of leaded gasoline. *Atmos. Environ.* **2004,** *38*, 1191-1200.
619 (55) Zhu, B. Q.; Chen, Y. W.; Peng, J. H. Lead isotope geochemistry of the urban environment in the
620 Pearl River Delta. *Appl. Geochem.* **2001,** *16*, 409-417.
621 (56) Bi, X. Y. **personal communication**.
622 (57) Duzgoren-Aydin, N. S. Sources and characteristics of lead pollution in the urban environment of
623 Guangzhou. *Sci. Total Environ.* **2007,** *385*, 182-195.
624 (58) Bi, C. J.; Zhou, Y.; Chen, Z. L.; Jia, J. P.; Bao, X. Y. Heavy metals and lead isotopes in soils, road
625 dust and leafy vegetables and health risks via vegetable consumption in the industrial areas of Shanghai,
626 China. *Sci. Total Environ.* **2018,** *619-620*, 1349-1357.
627 (59) Hu, X.; Zhang, Y.; Luo, J.; Xie, M. J.; Wang, T. J.; Lian, H. Z. Accumulation and quantitative
628 estimates of airborne lead for a wild plant (*Aster subulatus*). *Chemosphere* **2011,** *82*, 1351-1357.
629 (60) Chenery, S. R.; Izquierdo, M.; Marzouk, E.; Klinck, B.; Palumbo-Roe, B.; Tye, A. M. Soil–plant
630 interactions and the uptake of Pb at abandoned mining sites in the Rookhope catchment of the N.
631 Pennines, UK — A Pb isotope study. *Sci. Total Environ.* **2012,** *433*, 547-560.
632 (61) Notten, M. J. M.; Walraven, N.; Beets, C. J.; Vroon, P.; Rozema, J.; Aerts, R. Investigating the
633 origin of Pb pollution in a terrestrial soil–plant–snail food chain by means of Pb isotope ratios. *Appl.*
634 *Geochem.* **2008,** *23*, 1581-1593.
635 (62) Wong, C. S. C.; Li, X. D. Pb contamination and isotopic composition of urban soils in Hong Kong.
636 *Sci. Total Environ.* **2004,** *319*, 185-195.
637 (63) Farmer, J. G.; Broadway, A.; Cave, M. R.; Wragg, J.; Fordyce, F. M.; Graham, M. C.; Ngwenya,
638 B. T.; Bewley, R. J. F. A lead isotopic study of the human bioaccessibility of lead in urban soils from
639 Glasgow, Scotland. *Sci. Total Environ.* **2011,** *409*, 4958-4965.
640 (64) Shetaya, W. H.; Marzouk, E. R.; Mohamed, E. F.; Elkassas, M.; Bailey, E. H.; Young, S. D. Lead
641 in Egyptian soils: Origin, reactivity and bioavailability measured by stable isotope dilution. *Sci. Total*
642 *Environ.* **2018,** *618*, 460-468.
643 (65) Ha, H.; Olson, J. R.; Bian, L.; Rogerson, P. A. Analysis of heavy metal sources in soil using
644 Kriging interpolation on principal components. *Environ. Sci. Technol.* **2014,** *48*, 4999-5007.
645 (66) Rodríguez Martín, J. A.; Arias, M. L.; Grau Corbí, J. M. Heavy metals contents in agricultural
646 topsoils in the Ebro basin (Spain). Application of the multivariate geoestatistical methods to study spatial
647 variations. *Environ. Pollut.* **2006,** *144*, 1001-1012.
648 (67) Miner, D. K. Automotive hydraulic brake tube: the case for 90-10 copper-nickel tubing. *SAE*
649 *Technical Paper* **1993**, Report No. SAE 931028.
650 (68) Calvo, A. I.; Alves, C.; Castro, A.; Pont, V.; Vicente, A. M.; Fraile, R. Research on aerosol sources
651 and chemical composition: Past, current and emerging issues. *Atmos. Res.* **2013,** *120*, 1-28.
652 (69) Brock, C. A. Particle growth in urban and industrial plumes in Texas. *J. Geophys. Res.* **2003,** *108*.
653 (70) Bermudez, G. M.; Moreno, M.; Invernizzi, R.; Pla, R.; Pignata, M. L. Heavy metal pollution in
654 topsoils near a cement plant: the role of organic matter and distance to the source to predict total and hcl-
655 extracted heavy metal concentrations. *Chemosphere* **2010,** *78*, 375-81.
656 (71) Aelion, C. M.; Davis, H. T.; McDermott, S.; Lawson, A. B. Soil metal concentrations and toxicity:
657 Associations with distances to industrial facilities and implications for human health. *Sci. Total Environ.*
658 **2009,** *407*, 2216-2223.
659 (72) Martley, E.; Gulson, B. L.; Pfeifer, H. R. Metal concentrations in soils around the copper smelter
660 and surrounding industrial complex of Port Kembla, NSW, Australia. *Sci. Total Environ.* **2004,** *325*, 113-
661 127.

(73) Zhang, H.; Wang, Z.; Zhang, Y.; Ding, M.; Li, L. Identification of traffic-related metals and the effects of different environments on their enrichment in roadside soils along the Qinghai-Tibet highway. *Sci. Total Environ.* **2015,** *521-522*, 160-72.

(74) Carrero, J. A.; Arrizabalaga, I.; Bustamante, J.; Goienaga, N.; Arana, G.; Madariaga, J. M. Diagnosing the traffic impact on roadside soils through a multianalytical data analysis of the concentration profiles of traffic-related elements. *Sci. Total Environ.* **2013,** *458-460*, 427-434.

(75) Chen, X.; Xia, X. H.; Zhao, Y.; Zhang, P. Heavy metal concentrations in roadside soils and correlation with urban traffic in Beijing, China. *J. Hazard. Mater.* **2010,** *181*, 640-646.

671 Table 1 Metal concentrations (mg kg^{-1}) in different environmental compartments, and background values.

Sample (n)		Co	Cr	Cu	Ni	Pb	Zn	Al	Fe	Mn
Surface soils (180)	Mean±SD	8.60±3.34	54.8±29.5	44.1±32.9	24.2±17.4	57.4±30.4	153±99.4	39277±15315	22759±6286	347±306
	Median	7.94	48.7	35.2	20.2	49.4	126	37880	22039	296
	Range	2.75-18.2	17.0-283	4.90-209	7.86-201	14.5-212	31.9-671	5708-85865	6917-42107	8-3405
Road dust (178)	Mean±SD	6.90±1.76	64.3±49.9	102±78.6	23.6±11.2	84.1±41.2	384±164	12055±5506	21184±8459	411±482
	Median	6.67	55.4	80.1	20.8	76.2	361	10669	19257	299
	Range	3.77-14.0	15.1-498	20.5-438	9.20-88.8	25.6-280	87.9-992	5458-40355	11607-82703	126-4907
Foliar dust (160) [a]	Mean±SD	8.09±3.97	129±77.1	225±126	40.8±25.4	216±277	744±731	13125±9293	15401±9725	
	Median	7.51	115	201	34.8	165	563	10568	12554	
	Range	1.21-21.7	7.66-541	47.2-895	3.73-192	33.6-3024	72-7533	2253-66826	2999-53151	
Washed leaves (160)	Mean±SD	0.16±0.03	1.04±0.47	6.9±1.71	0.70±0.26	2.37±2.83	20.8±5.92	246±176	289±184	
	Median	0.16	0.98	6.68	0.65	1.68	19.9	198	235	
	Range	0.09-0.28	0.11-3.10	3.83-13.3	0.26-2.24	0.24-26.7	11.3-45.9	41-1260	55-1000	
Guangzhou background soil [b]		6.3	39	10.4	12.3	41	58	56153	15737	235

a: Mn concentrations were not shown because most of the Mn concentration of tree leaves were below the detection limit; b: Guangdong Geological Survey [31].

672

673

674 Table 2 Summary of Pb isotopic compositions (mean (minimum-maximum)) of the samples.

Sample (n=40)	$^{204}Pb/^{207}Pb$	$^{206}Pb/^{207}Pb$	$^{208}Pb/^{207}Pb$
Surface soil (n=10)	0.0636 (0.0633-0.0639)	1.1815 (1.1678-1.2016)	2.4675 (2.4506-2.4897)
Road dust (n=10)	0.0638 (0.0636-0.0640)	1.1672 (1.1521-1.1755)	2.4527 (2.4381-2.4627)
Unwashed leaf (n=10)	0.0639 (0.0637-0.0641)	1.1704 (1.1677-1.1738)	2.4493 (2.4416-2.4633)
Washed leaf (n=10)	0.0639 (0.0636-0.0643)	1.1710 (1.1670-1.1762)	2.4462 (2.4357-2.4645)

675

676 **Figure captions**

677 **Figure 1** Trace metal concentrations of environmental compartments in different land
678 use areas including the sample numbers listed below the x-axis. The box represents the
679 data between the 25^{th} and 75^{th} percentiles. The small square and horizontal line within
680 the box indicates the mean and median data, respectively. The whiskers (error bars)
681 above and below the box indicate the 95^{th} and 5^{th} percentiles, respectively. The asterisks
682 indicate the 1^{st} and 99^{th} percentile.

683 **Figure 2** Impact of the steel factory (a-b) and power plant (c-d) on the Pb and Zn
684 concentrations in the foliar dust. The *x*-axis indicates increasing distance from the
685 industrial source. Pearson's r and *p* values were listed in the figures.

686 **Figure 3** Distribution of Cu, Pb, and Zn concentrations (mg kg^{-1}) in the surface soil (a-
687 c), road dust (d-f), and foliar dust (g-i). The area with highest population density [43]
688 and dense traffic network (Figure S6) was circled in red in (d).

689 **Figure 4** Lead isotopic compositions ($^{206}Pb/^{207}Pb$ vs. $^{208}Pb/^{207}Pb$) of different urban
690 compartments. Data for possible Pb sources [16, 24, 51-56] were included in (a) for
691 comparison. All data in the dashed rectangle in (a) are enlarged in (b) and Pb isotopic
692 compositions of coals and traffic sources are aggregated in (b). The red line in (b) was
693 obtained from the linear regression of road dust samples of this study and unleaded
694 samples from literatures [16, 52-54] with R^2=0.96. Detailed information is listed in
695 Tables S5 and S6.

696 **Figure 5** Spatial variation in traffic contributions (PC2, a–c) and industrial
697 contributions (PC3, d–f) to Cu, Pb, and Zn in road dust and foliar dust, respectively.
698 The area with highest population density [43] and dense traffic network (Figure S6)
699 was circled in red in a (Cu). In the road dust, PC2 was the single independent variable
700 in the APCS-MLR model for Cu, indicating the predominant source of Cu in road dust
701 from traffic activities.

702 **Figure 6** Scheme for trace metal sources and cycling in urban compartments including

surface soil, road dust, and foliar dust in the megacity Guangzhou. The arrows indicate the transport of trace metals from sources, such as lithogenic sources, industrial emission/coal combustion, traffic exhaust/industrial transport, orchard activity, atmospheric deposition, particle resuspension from surface soil and road dust, and other anthropogenic sources. The numbers are the ranges of certain sources contributing to the trace metals in each terrestrial urban compartment obtained using APCS-MLR modeling.

710

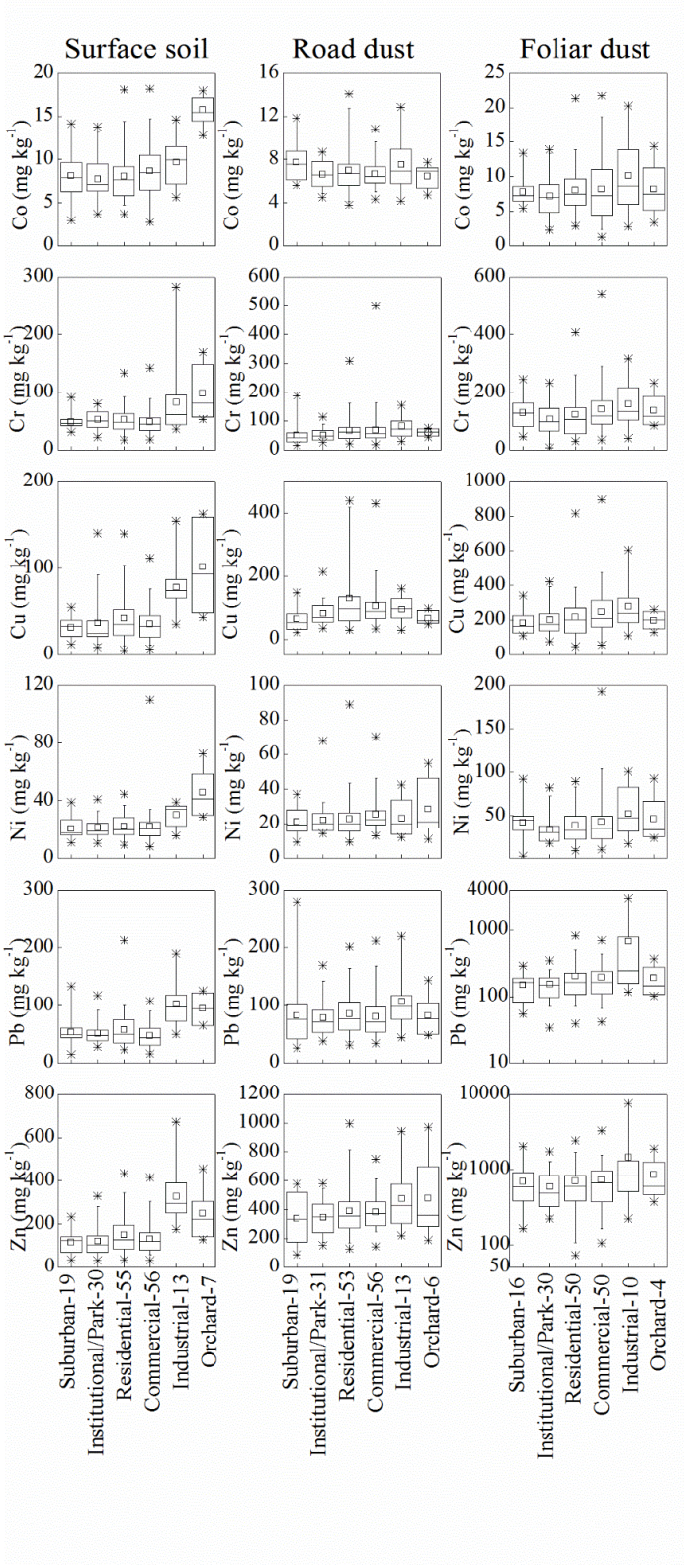

711

712 Figure 1

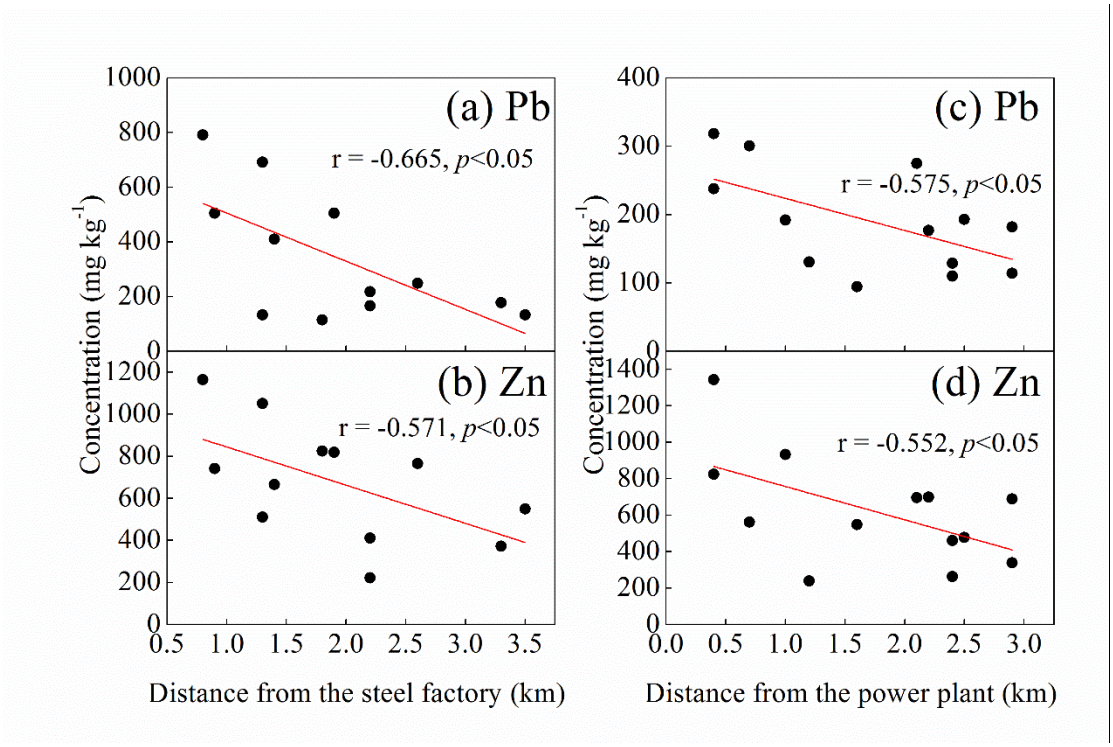
(a) Pb
r = -0.665, p<0.05
(b) Zn
r = -0.571, p<0.05
(c) Pb
r = -0.575, p<0.05
(d) Zn
r = -0.552, p<0.05
Concentration (mg kg-1)
Concentration (mg kg-1)
Distance from the steel factory (km)
Distance from the power plant (km)

Figure 2

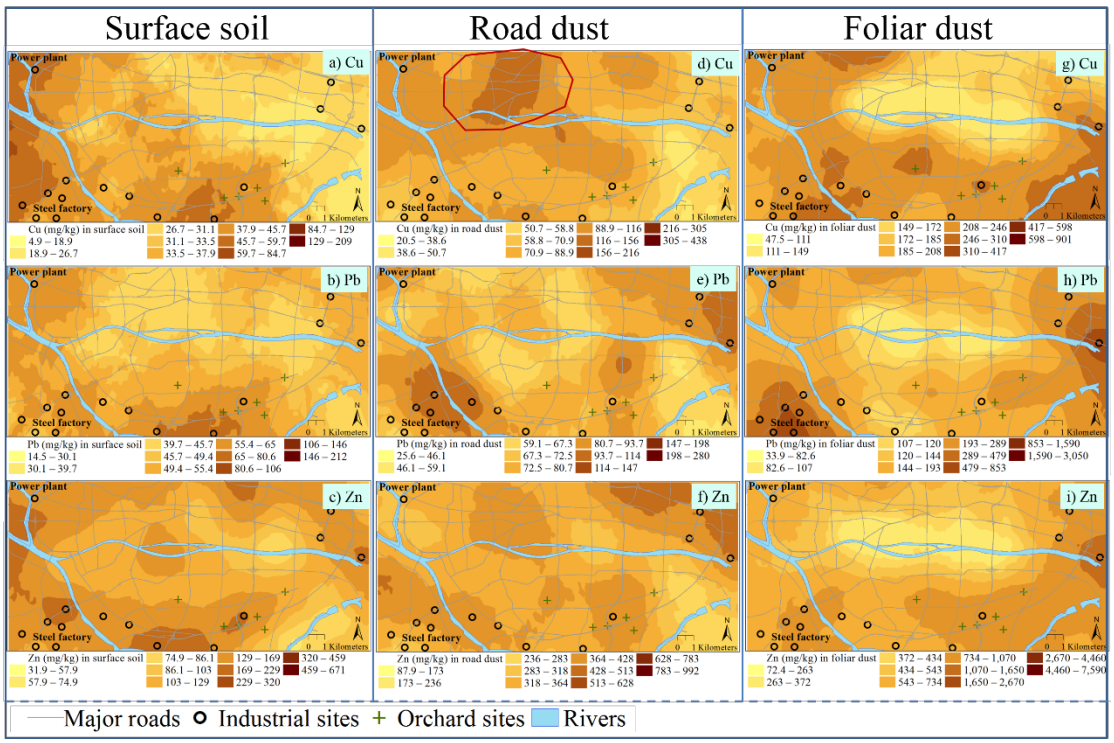
Surface soil
Road dust
Foliar dust
a) Cu
b) Pb
c) Zn
d) Cu
e) Pb
f) Zn
g) Cu
h) Pb
i) Zn
Power plant
Steel factory
Cu (mg/kg) in surface soil
4.9 – 18.9
18.9 – 26.7
26.7 – 31.1
31.1 – 33.5
33.5 – 37.9
37.9 – 45.7
45.7 – 59.7
59.7 – 84.7
84.7 – 129
129 – 209
Pb (mg/kg) in surface soil
14.5 – 30.1
30.1 – 39.7
39.7 – 45.7
45.7 – 49.4
49.4 – 55.4
55.4 – 65
65 – 80.6
80.6 – 106
106 – 146
146 – 212
Zn (mg/kg) in surface soil
31.9 – 57.9
57.9 – 74.9
74.9 – 86.1
86.1 – 103
103 – 129
129 – 169
169 – 229
229 – 320
320 – 459
459 – 671
Cu (mg/kg) in road dust
20.5 – 38.6
38.6 – 50.7
50.7 – 58.8
58.8 – 70.9
70.9 – 88.9
88.9 – 116
116 – 156
156 – 216
216 – 305
305 – 438
Pb (mg/kg) in road dust
25.6 – 46.1
46.1 – 59.1
59.1 – 67.3
67.3 – 72.5
72.5 – 80.7
80.7 – 93.7
93.7 – 114
114 – 147
147 – 198
198 – 280
Zn (mg/kg) in road dust
87.9 – 173
173 – 236
236 – 283
283 – 318
318 – 364
364 – 428
428 – 513
513 – 628
628 – 783
783 – 992
Cu (mg/kg) in foliar dust
47.5 – 111
111 – 149
149 – 172
172 – 185
185 – 208
208 – 246
246 – 310
310 – 417
417 – 598
598 – 901
Pb (mg/kg) in foliar dust
33.9 – 82.6
82.6 – 107
107 – 120
120 – 144
144 – 193
193 – 289
289 – 479
479 – 853
853 – 1,590
1,590 – 3,050
Zn (mg/kg) in foliar dust
72.4 – 263
263 – 372
372 – 434
434 – 543
543 – 734
734 – 1,070
1,070 – 1,650
1,650 – 2,670
2,670 – 4,460
4,460 – 7,590
0 1 Kilometers
Major roads
Industrial sites
Orchard sites
Rivers

Figure 3

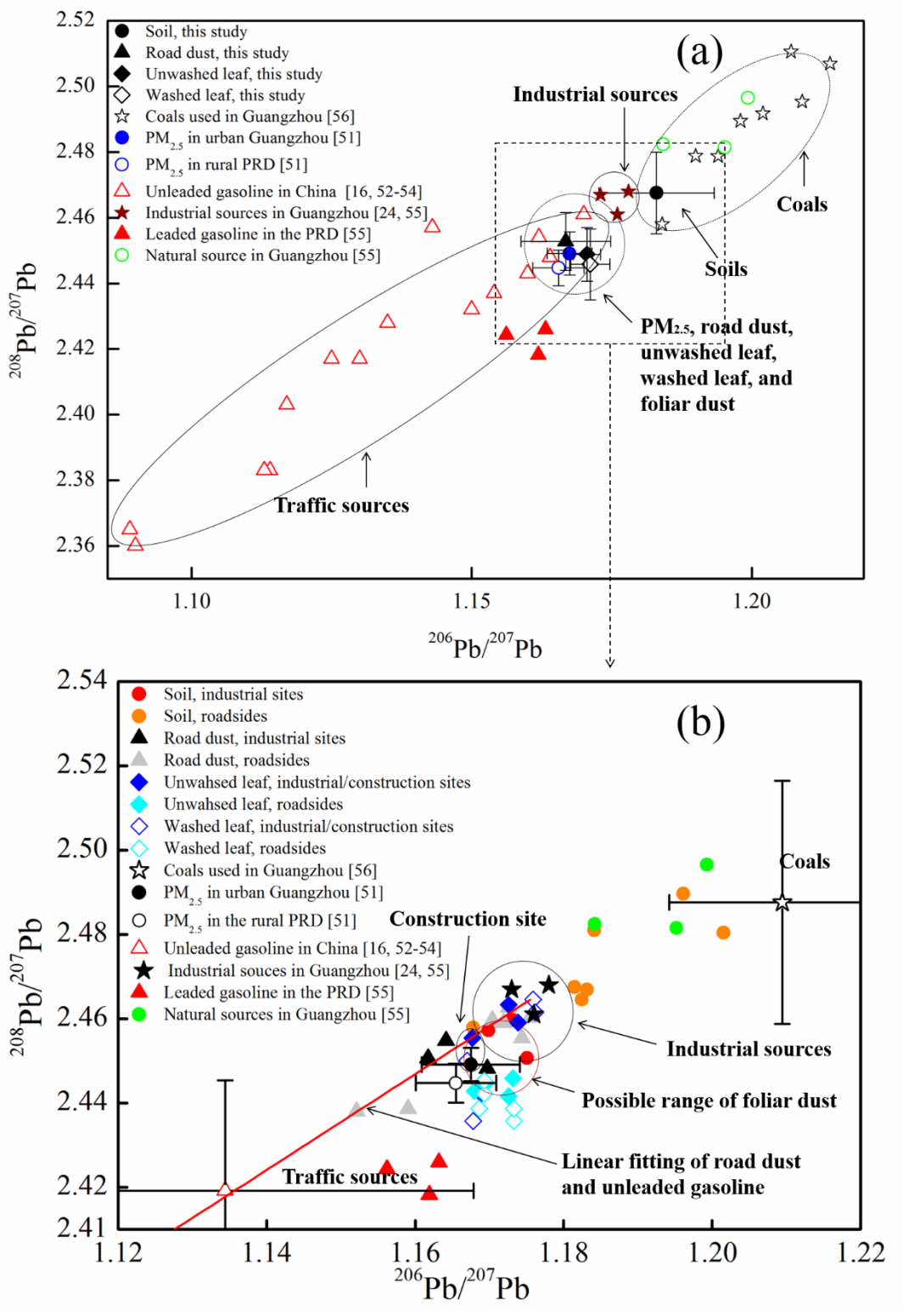

721

722 Figure 4

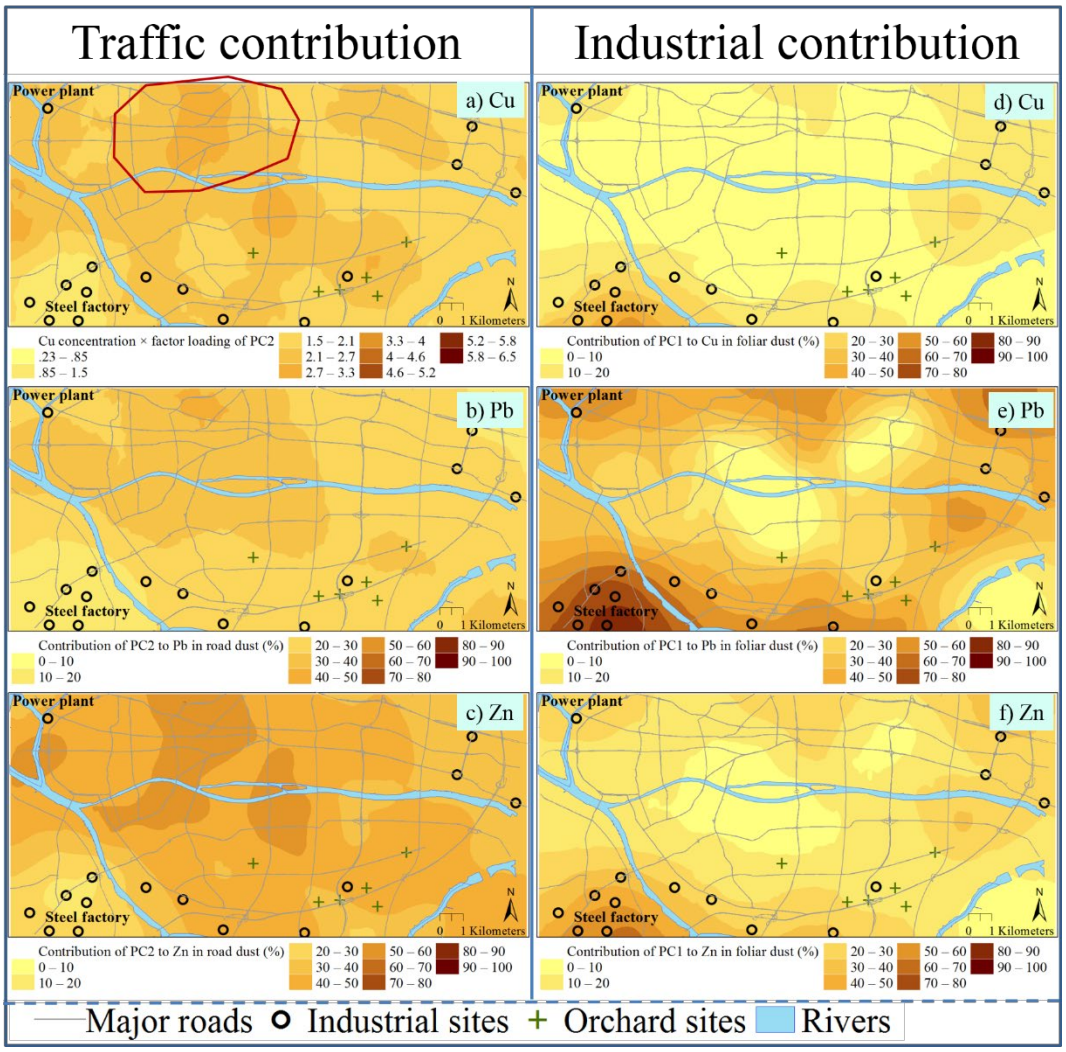
Traffic contribution
Industrial contribution
Power plant
Steel factory
a) Cu
b) Pb
c) Zn
d) Cu
e) Pb
f) Zn
0 1 Kilometers
N
Cu concentration × factor loading of PC2
.23 – .85
.85 – 1.5
1.5 – 2.1
2.1 – 2.7
2.7 – 3.3
3.3 – 4
4 – 4.6
4.6 – 5.2
5.2 – 5.8
5.8 – 6.5
Contribution of PC2 to Pb in road dust (%)
Contribution of PC2 to Zn in road dust (%)
Contribution of PC1 to Cu in foliar dust (%)
Contribution of PC1 to Pb in foliar dust (%)
Contribution of PC1 to Zn in foliar dust (%)
0 – 10
10 – 20
20 – 30
30 – 40
40 – 50
50 – 60
60 – 70
70 – 80
80 – 90
90 – 100
Major roads
Industrial sites
Orchard sites
Rivers

Figure 5

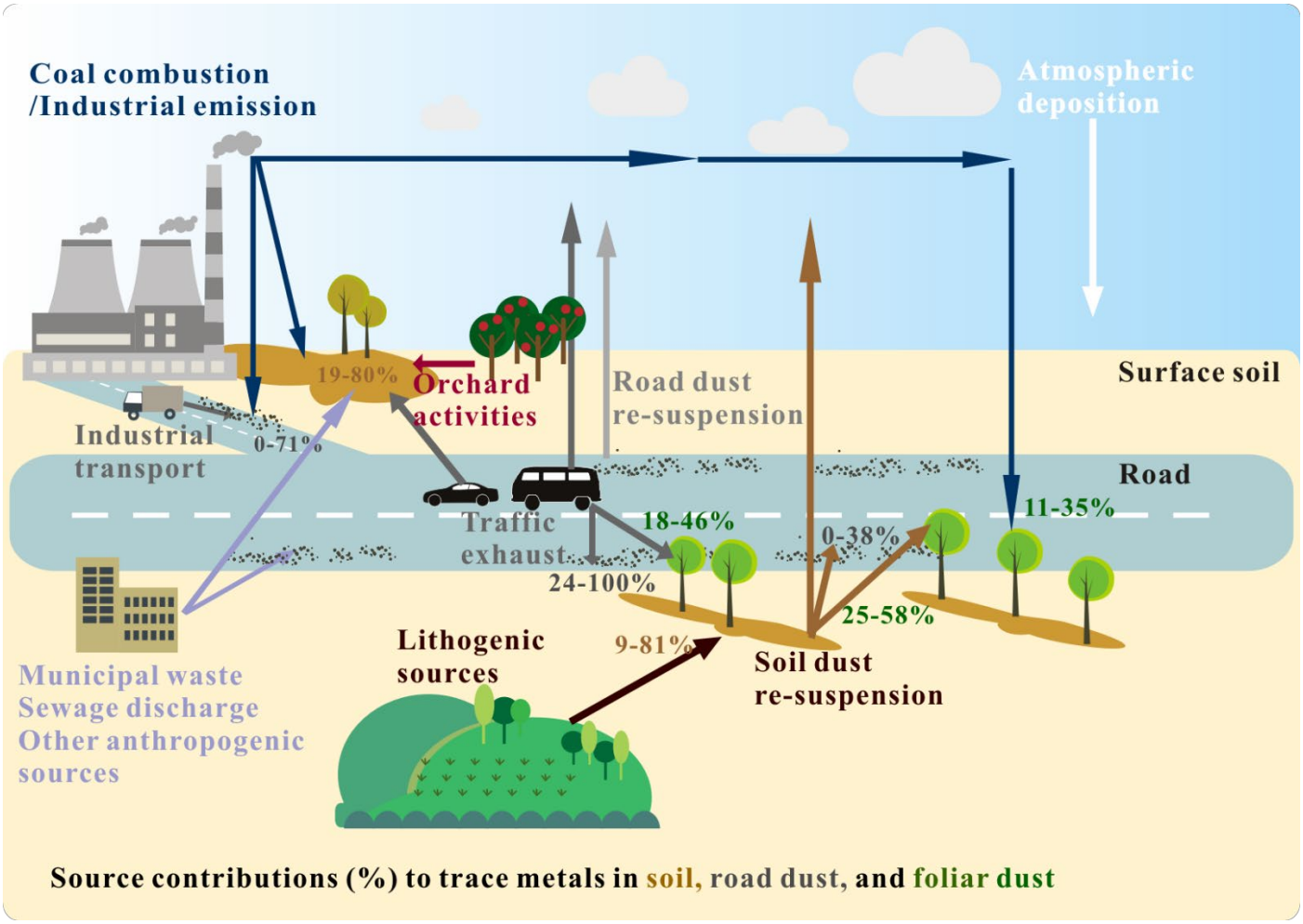
Coal combustion
/Industrial emission
Atmospheric
deposition
Surface soil
19-80%
Orchard
activities
Road dust
re-suspension
Industrial
transport
0-71%
Road
Traffic
exhaust
18-46%
0-38%
11-35%
24-100%
25-58%
Lithogenic
sources
9-81%
Soil dust
re-suspension
Municipal waste
Sewage discharge
Other anthropogenic
sources
Source contributions (%) to trace metals in soil, road dust, and foliar dust

Figure 6